

## The Unique Type Ib Supernova 2005bf: A WN Star Explosion Model for Peculiar Light Curves and Spectra

N. Tominaga<sup>1</sup>, M. Tanaka<sup>1</sup>, K. Nomoto<sup>1,2</sup>, P.A. Mazzali<sup>1,2,3,4</sup>, J. Deng<sup>5</sup>, K. Maeda<sup>6</sup>, H. Umeda<sup>1</sup>, M. Modjaz<sup>7</sup>, M. Hicken<sup>7</sup>, P. Challis<sup>7</sup>, R.P. Kirshner<sup>7</sup>, W.M. Wood-Vasey<sup>7</sup>, C.H. Blake<sup>7</sup>, J.S. Bloom<sup>8</sup>, M.F. Skrutskie<sup>9</sup>, A. Szentgyorgyi<sup>7</sup>, E.E. Falco<sup>7</sup>, N. Inada<sup>10</sup>, T. Minezaki<sup>10</sup>, Y. Yoshii<sup>10</sup>, K. Kawabata<sup>11</sup>, M. Iye<sup>12</sup>, G.C. Anupama<sup>13</sup>, D.K. Sahu<sup>13</sup>, and T.P. Prabhu<sup>13</sup>

### ABSTRACT

Observations and modeling for the light curve (LC) and spectra of supernova (SN) 2005bf are reported. This SN showed unique features: the LC had two maxima, and declined rapidly after the second maximum, while the spectra showed strengthening He lines whose velocity increased with time. The double-peaked LC can be reproduced by a double-peaked <sup>56</sup>Ni distribution, with most <sup>56</sup>Ni at low velocity and a small amount at high velocity. The rapid post-maximum decline requires a large fraction of the  $\gamma$ -rays to escape from the <sup>56</sup>Ni-dominated region, possibly because of low-density “holes”. The presence of Balmer lines in the spectrum suggests that the He layer of the progenitor was substantially intact. Increasing  $\gamma$ -ray deposition in the He layer due to enhanced  $\gamma$ -ray escape from the <sup>56</sup>Ni-dominated region may explain both the delayed strengthening and the increasing velocity of the He lines. The SN has massive ejecta ( $\sim 6-7M_{\odot}$ ), normal kinetic energy ( $\sim 1.0-1.5 \times 10^{51}$  ergs), high peak bolometric luminosity ( $\sim 5 \times 10^{42}$  erg s<sup>-1</sup>) for an epoch as late as  $\sim 40$  days, and a large <sup>56</sup>Ni mass ( $\sim 0.32M_{\odot}$ ). These properties, and the presence of a small amount of H suggest that the progenitor was initially massive ( $M \sim 25-30M_{\odot}$ ) and had lost most of its H envelope, and was possibly a WN star. The double-peaked <sup>56</sup>Ni distribution suggests that the explosion may have formed jets that did not reach the He layer. The properties of SN 2005bf resemble those of the explosion of Cassiopeia A.

*Subject headings:* supernovae: general — supernovae: individual (SN 2005bf) — stars: Wolf-Rayet — supernovae: individual (Cassiopeia A)

---

<sup>1</sup>Department of Astronomy, School of Science, University of Tokyo, Bunkyo-ku, Tokyo 113-0033, Japan; tominaga@astron.s.u-tokyo.ac.jp, mtanaka@astron.s.u-tokyo.ac.jp, nomoto@astron.s.u-tokyo.ac.jp, umeda@astron.s.u-tokyo.ac.jp

<sup>2</sup>Research Center for the Early Universe, School of Science, University of Tokyo, Bunkyo-ku, Tokyo 113-0033, Japan

<sup>3</sup>Max-Planck Institut für Astrophysik, Karl-Schwarzschild Str. 1, D-85748 Garching, Germany; mazzali@MPA-Garching.MPG.DE

<sup>4</sup>Istituto Nazionale di Astrofisica-OATs, Via Tiepolo 11, I-34131 Trieste, Italy

<sup>5</sup>National Astronomical Observatories, CAS, 20A Datun Road, Chaoyang District, Beijing 100012, China;

---

jsdeng@bao.ac.cn

<sup>6</sup>Department of Earth Science and Astronomy, Graduate School of Arts and Science, University of Tokyo, Meguro-ku, Tokyo 153-8902, Japan; maeda@esa.c.u-tokyo.ac.jp

<sup>7</sup>Harvard-Smithsonian Center for Astrophysics, 60 Garden Street, Cambridge, MA, 02138, USA; mmodjaz@cfa.harvard.edu, mhicken@cfa.harvard.edu, pchallis@cfa.harvard.edu, kirshner@cfa.harvard.edu, wnwood-vasey@cfa.harvard.edu, cblake@cfa.harvard.edu, saint@cfa.harvard.edu, efalco@cfa.harvard.edu

<sup>8</sup>Department of Astronomy, University of California Berkeley, 601 Campbell Hall, Berkeley, CA 94720, USA; jlbloom@astro.berkeley.edu

<sup>9</sup>Department of Astronomy, University of Virginia,

## 1. INTRODUCTION

As the sample of well-studied supernovae (SN) grows, it is not surprising that rare types are observed. At first, these may seem strange and unique; in time they may become well-understood subtypes. We believe that SN 2005bf is one of these new types: it has unique photometric and spectroscopic behavior. Based on a successful effort to model our light curve and spectra, we believe that SN 2005bf fits into the scheme suggested by Nomoto et al. (1995) which places core-collapse SN in a sequence (IIP-IIL-Ib-Ic) of increasing mass loss from the progenitor star.

Discovered by Monard (2005) and Moore & Li (2005) on April 6, 2005 (UT) in the spiral arms of the SBb galaxy MCG +00-27-5, SN 2005bf was initially classified as a Type Ic SN (SN Ic) (Morell et al. 2005; Modjaz et al. 2005a). The later development of He lines suggested an unprecedented transition to Type Ib (Wang & Baade 2005; Modjaz et al. 2005b). Even stranger, the light curve was very different from any known SN (Hamuy et al. 2005): a fairly rapid rise to a first peak was followed by a period of stalling or slow decline and by a new rise to a later, brighter peak at  $\sim 40$  days after explosion (Fig. 1). The brightness ( $M_{\text{bol}} \sim -18$  mag) and the late epoch of the second peak suggest this SN ejected a large amount of  $^{56}\text{Ni}$ . SN 2005bf does not show the broad lines seen in hypernovae. These properties make SN 2005bf a very interesting SN.

Photometry was obtained in  $UBVR'i'$  bands at the 1.2m telescope at the Fred Lawrence Whipple Observatory on Mt. Hopkins (FLWO; Modjaz et al. 2005c),  $JHK_s$  bands at the refurbished 1.3m telescope on Mt. Hopkins (PAIRI-

TEL; <http://pairitel.org>; Modjaz et al. 2005c) at FLWO,  $BVRI$  bands at the Himalayan Chandra Telescope (HCT; Anupama et al. 2005), and  $BVRIJHK$  bands at the MAGNUM Telescope (Yoshii et al. 2003; Inada et al. 2005) (Fig. 1). Spectroscopic observations were made at FLWO, HCT and the SUBARU Telescope (Kawabata et al. 2002, 2005). We used the light curve and spectra to constrain models for the SN and to infer the properties of the progenitor star<sup>14</sup>.

## 2. LIGHT CURVE MODELS

The bolometric light curve (LC) was constructed as in Yoshii et al. (2003; see Fig. 2). Synthetic bolometric LCs were computed with an LTE radiation hydrodynamics code and a gray  $\gamma$ -ray transfer code (Iwamoto et al. 2000). Electron-scattering and line opacity were considered for radiation transport. The former used the ionization computed with the Saha equation. For the latter the approximate formula given in Mazzali et al. (2001) was adopted, with modifications to account for the C, O, and He-rich layers. We assumed a Galactic reddening  $E(B - V) = 0.045$ , a distance modulus  $\mu = 34.5$  (Schlegel, Finkbeiner, & Davis 1998; <http://nedwww.ipac.caltech.edu/index.html>; Falco et al. 1999), and an explosion date of 2005 March 28 UT as inferred from the marginal detection on 2005 March 30 UT (Moore & Li 2005).

The LC is powered by the radioactive decay of  $^{56}\text{Ni}$  to  $^{56}\text{Co}$  and  $^{56}\text{Fe}$ . The theoretical LC width near peak depends on ejected mass  $M_{\text{ej}}$  and explosion kinetic energy  $E$  as  $M_{\text{ej}}E^{-3}$  (Arnett 1982; Nomoto et al. 2004). The mass and distribution of  $^{56}\text{Ni}$  are constrained by the LC brightness and shape, but various combinations of  $(M_{\text{ej}}, E)$  can fit the LC. Spectra break this degeneracy and help establish the abundance distribution in the ejecta.

The density structure used for the LC calculation was based on the C+O star model CO138E50 used for SN 1998bw (Nakamura et al. 2001) but rescaled by changing  $r$ ,  $v$ , and  $\rho$  such that  $M_{\text{ej}}$  and  $E$  are rescaled as  $M_{\text{ej}} \propto \rho r^3$  and  $E \propto \rho v^2 r^3$ ,

---

Charlottesville, VA 22903, USA; mfs4n@virginia.edu

<sup>10</sup>Institute of Astronomy, School of Science, University of Tokyo, 2-21-1 Osawa, Mitaka, Tokyo 181-0015, Japan; inada@ioa.s.u-tokyo.ac.jp, minezaki@mtk.ioa.s.u-tokyo.ac.jp, yoshii@mtk.ioa.s.u-tokyo.ac.jp

<sup>11</sup>Hiroshima Astrophysical Science Center, Hiroshima University, Hiroshima 739-8526, Japan; kawabtkj@hiroshima-u.ac.jp

<sup>12</sup>Optical and Infrared Astronomy Division, National Astronomical Observatory of Japan, 2-21-1 Osawa, Mitaka, Tokyo 181-8588, Japan; iye@optik.mtk.nao.ac.jp

<sup>13</sup>Indian Institute of Astrophysics, Koramangala, Bangalore 560 034, India; gca@iiap.res.in, dks@crest.ernet.in, tpp@iiap.res.in

<sup>14</sup>After this paper was submitted and placed on astro-ph, the Carnegie Supernova Project and their collaborators placed a paper on SN 2005bf on astro-ph (Folatelli et al. 2005). It is beyond the scope of this Letter to compare the observations and theoretical models in detail.

respectively. The He distribution is constrained by observational evidence and spectral fitting, as discussed in §3.

The He absorption lines first appeared at a velocity of  $\sim 6,000 \text{ km s}^{-1}$ . The velocity increased slowly with time, reaching  $\sim 7,000 \text{ km s}^{-1}$  (Fig. 3), an unusual behavior for SN Ib (see, e.g., Branch et al 2002). On the contrary, the velocities of the Fe lines declined with time.  $\text{H}\alpha$ , and possibly  $\text{H}\beta$  and  $\text{H}\gamma$ , were detected (Wang & Baade 2005; Anupama et al. 2005), as possibly in other SN Ib (Deng et al. 2000; Branch et al. 2002). The weakness of these lines suggests a small H mass (see §3), so we assumed that H did not affect the LC. Seeing traces of H suggests that the He layer was fairly intact before the explosion, so we included it in our LC computation. We assumed that He is mainly above  $v \gtrsim 6,000 \text{ km s}^{-1}$ , as suggested by the observed He line velocity. The light curve for a model with  $M_{\text{ej}} = 7M_{\odot}$  and  $E_{51} = E/10^{51} \text{ ergs} = 2.1$  is shown as a dashed line in Figure 2.

The model WR star explosion of Ensmann & Woosley (1988) produced a double-peaked LC, but in that case the first peak was caused by recombination of He ionized by shock heating, and is too narrow for the first peak of the light curve of SN 2005bf, which has a width of  $\sim 15$  days. The only possibility we found to reproduce the double-peaked LC was to assume a distribution with most  $^{56}\text{Ni}$  at low velocity, and a small amount at high velocity, as follows:  $(X(^{56}\text{Ni}), M(^{56}\text{Ni})/M_{\odot}) = (0.75, 0.18)$  at  $v \lesssim 1,600 \text{ km s}^{-1}$ ,  $(0.015, 0.04)$  at  $v \sim 1,600 - 3,900 \text{ km s}^{-1}$ ,  $(0.025, 0.07)$  at  $v \sim 3,900 - 6,200 \text{ km s}^{-1}$ , and no  $^{56}\text{Ni}$  at  $v \gtrsim 6,200 \text{ km s}^{-1}$ . Here  $X$  denotes the mass fraction. The total  $^{56}\text{Ni}$  mass is  $M(^{56}\text{Ni}) = 0.29M_{\odot}$ . The first peak of the LC is powered by a small amount of high-velocity  $^{56}\text{Ni}$  at  $v \gtrsim 3,900 \text{ km s}^{-1}$ . The second peak is powered by  $^{56}\text{Ni}$  in the low velocity central region. The outer extent of the outer ( $v \sim 6,200 \text{ km s}^{-1}$ ) and inner ( $v \sim 1,600 \text{ km s}^{-1}$ )  $^{56}\text{Ni}$  are well determined from the time of the first and second peak, but the inner distribution of the outer  $^{56}\text{Ni}$  is not well constrained, since it has little effect on the light curve.

The large amount of  $^{56}\text{Ni}$  ( $\sim 0.29M_{\odot}$ ) would ordinarily lead to a bright  $^{56}\text{Co}$  tail. The dashed line in Figure 2 shows a LC computed with a  $\gamma$ -ray

opacity  $\kappa_{\gamma} = 0.027 \text{ cm}^2 \text{ g}^{-1}$  (Shigeyama & Nomoto 1990). However, the observed LC continued to decline rapidly, suggesting that  $\gamma$ -rays escape more easily from SN 2005bf than in the typical case. We used a reduced  $\gamma$ -ray opacity to simulate this situation.

Using  $\kappa_{\gamma} = 0.001 \text{ cm}^2 \text{ g}^{-1}$  at  $v < 5,400 \text{ km s}^{-1}$  (but keeping  $\kappa_{\gamma} = 0.027 \text{ cm}^2 \text{ g}^{-1}$  at  $v > 5,400 \text{ km s}^{-1}$ ), we obtained a set of models with  $(M_{\text{ej}}/M_{\odot}, E_{51}) = (5, 0.6), (6, 1.0), (7, 1.3), (8, 1.7), (9, 2.3), (10, 2.8),$  and  $(11, 3.3)$  that reproduce the light curve. The models with  $M_{\text{ej}} = 6 - 7M_{\odot}$  best fit the spectra (§3). The solid line in Figure 2 shows the LC with  $M_{\text{ej}} = 7M_{\odot}$ ,  $E_{51} = 1.3$ ,  $M(^{56}\text{Ni}) = 0.32M_{\odot}$ , and the following  $^{56}\text{Ni}$  distribution:  $(X(^{56}\text{Ni}), M(^{56}\text{Ni})/M_{\odot}) = (0.44, 0.22)$  at  $v \lesssim 1,600 \text{ km s}^{-1}$ ,  $(0.013, 0.04)$  at  $v \sim 1,600 - 3,900 \text{ km s}^{-1}$ ,  $(0.03, 0.06)$  at  $v \sim 3,900 - 5,400 \text{ km s}^{-1}$ , and no  $^{56}\text{Ni}$  at  $v \gtrsim 5,400 \text{ km s}^{-1}$ .

Enhanced  $\gamma$ -ray escape could result from the presence of low-density “holes”. Such a structure may be produced by jets and Rayleigh-Taylor instabilities possibly caused by magnetar activity (see §4). While  $\gamma$ -rays could escape much more easily from the low-density holes, those  $\gamma$ -rays that are trapped in the high-density region are converted to optical photons. Thus optical photons are selectively produced in high density regions, where the optical opacity can be expected to be normal.

Because of the smaller average  $\kappa_{\gamma}$  in the  $^{56}\text{Ni}$  region and the enhanced escape of  $\gamma$ -rays with respect to a model with normal  $\kappa_{\gamma}$ , more  $^{56}\text{Ni}$  is necessary to power the LC, but lower velocity  $^{56}\text{Ni}$  (i.e.,  $v \lesssim 5,400 \text{ km s}^{-1}$ ) can reproduce the first peak. In other words,  $^{56}\text{Ni}$  is mixed out but does not reach the He layer at  $v \gtrsim 6,000 \text{ km s}^{-1}$ . Such a double-peaked distribution of  $^{56}\text{Ni}$  might be produced by jets that did not reach the He layer.

### 3. SPECTROSCOPIC MODELS

We computed synthetic spectra from the explosion models described above. The comparison with the observed spectra is necessary to distinguish among the models. We used the Monte-Carlo spectrum synthesis code described in Mazzali & Lucy (1993), Lucy (1999), and Mazzali (2000). Since the code does not take into account non-thermal processes, which are essential to pop-

ulate He I levels (Lucy 1991), we introduced a “non-thermal factor” (Harkness et al. 1987) to reproduce the He lines. This parameterized factor, denoted as  $f$ , represents the degree of departure from the level populations computed using a modified nebular approximation, and is used to multiply all He I line opacities.

Our synthetic spectra are compared to the observed ones in Figure 4. The bolometric luminosities used to fit the spectra agree with the observed ones within 10%. The model with  $(M_{\text{ej}}/M_{\odot}, E_{51}) = (7, 1.3)$  provides satisfactory fits for all spectra. The photospheric velocities this model predicts agree with those used to fit the spectra within 20%.

At the time of the first peak (UT April 13, 16 days after explosion; Modjaz et al. 2005c) SN 2005bf exhibited SN Ic features, but actually both He and H can be distinguished. The feature near  $5700\text{\AA}$  is probably He I  $5876\text{\AA}$ . We obtained a good fit for this spectrum with a bolometric luminosity  $L = 2.0 \times 10^{42} \text{ erg s}^{-1}$  and a photospheric velocity  $v_{\text{ph}} = 6,200 \text{ km s}^{-1}$ . The non-thermal factor was set to 1. The model with  $M_{\text{ej}} = 7M_{\odot}$  fits better than that with  $M_{\text{ej}} = 6M_{\odot}$ . The feature at  $6300\text{\AA}$  is reproduced as a blend of H $\alpha$  and Si II  $6355\text{\AA}$  (Fig. 4, inset). The core of the line cannot be due to Si II because this would require a Si velocity of  $\sim 5,000 \text{ km s}^{-1}$ , which is smaller than the photospheric velocity. It can, however, be reproduced as H $\alpha$  if  $\sim 0.02M_{\odot}$  of H is present above  $v \gtrsim 13,000 \text{ km s}^{-1}$ .

Near maximum brightness (UT May 4, 37 days after explosion) He lines become conspicuous. The model has  $L = 5.0 \times 10^{42} \text{ erg s}^{-1}$ ,  $v_{\text{ph}} = 4,600 \text{ km s}^{-1}$ , and  $f = 2.0 \times 10^3$  (only at  $v \gtrsim 6,500 \text{ km s}^{-1}$ ). Most features, including Ca II, Fe II and Mg II are also well reproduced. The line near  $6300\text{\AA}$  is reproduced as Si II ( $6355\text{\AA}$ ) at this epoch: the photospheric velocity is low enough for Si to be above the photosphere, while the H layer is too far above the photosphere to produce an absorption. For a spectrum on UT May 16th (49 days, Kawabata et al. 2005), we also obtain a reasonable fit with parameters  $L = 3.8 \times 10^{42} \text{ erg s}^{-1}$ ,  $v_{\text{ph}} = 3,800 \text{ km s}^{-1}$ , and  $f = 2 \times 10^6$  (at  $v \gtrsim 7,200 \text{ km s}^{-1}$ ).

These values of the “non-thermal factor” compare well with the results of detailed calculations

(Lucy 1991), although the value at the last epoch appears too large. To mimic the increasing velocity of He I  $\lambda 5876$ , we introduced the non-thermal factor at increasingly high velocity at more advanced epochs. Enhanced  $\gamma$ -ray escape from the  $^{56}\text{Ni}$ -dominated region can yield rapidly increasing  $\gamma$ -ray deposition in the He layer and higher He excitation, as confirmed by the fact that the  $\gamma$ -ray deposition rates derived from the LC calculations increase gradually over time at  $7,200 \text{ km s}^{-1}$ . The ratios between the deposition at  $7,200 \text{ km s}^{-1}$  49 days and 16 days after the explosion is 14.5 (for comparison it is 4.6 at  $6,200 \text{ km s}^{-1}$ ). As the optical depth of the He lines increases, the region where they become optically thick (and where the non-thermal factor is applied) moves to higher velocity.

#### 4. CONCLUSIONS & DISCUSSION

We have studied the properties of SN 2005bf by modelling the light curve and the spectra. Our best fit model has  $M_{\text{ej}} \sim 7M_{\odot}$  and  $E_{51} \sim 1.3$ . The ejecta consist of  $^{56}\text{Ni}$  ( $\sim 0.32M_{\odot}$ ), He ( $\sim 0.4M_{\odot}$ ), intermediate mass elements (mainly O, Si, S), and a small amount of H ( $\sim 0.02M_{\odot}$ ). Thus the progenitor had lost almost all its H envelope, but retained most of the He-rich layer, as in WN stars. The double-peaked light curve is reproduced by a double-peaked  $^{56}\text{Ni}$  distribution: such a distribution may be caused by jets that did not reach the He layer. Strong He lines were not seen in the earliest spectra because radioactive  $^{56}\text{Ni}$  was too far from the He layer to excite He atoms. Increasing  $\gamma$ -ray deposition in the He layer due to enhanced  $\gamma$ -ray escape from the  $^{56}\text{Ni}$ -dominated region may explain both the delayed strengthening and the increasing velocity of the He lines.

The He core mass at explosion was  $M_{\text{He}} = M_{\text{ej}} + M_{\text{cut}} \sim 7.5 - 8.5M_{\odot}$ . The progenitor was probably a WN star of main-sequence mass  $M_{\text{MS}} \sim 25 - 30M_{\odot}$  (Nomoto & Hashimoto 1988; Umeda & Nomoto 2005). The formation of a WN star from a star of only  $\sim 25M_{\odot}$  suggests that rotation may have been important (Hirschi, Meynet & Maeder 2005), although not sufficient to make SN 2005bf a hypernova.

Our model requires the production of an unusually large amount of  $^{56}\text{Ni}$  but a normal explosion energy. To examine whether this is pos-

sible, we performed hydrodynamical simulations of explosive nucleosynthesis for the model with  $M_{\text{MS}} = 25M_{\odot}$  and  $E_{51} = 1.3$  as in Umeda & Nomoto (2005). In order to produce  $\sim 0.32M_{\odot}$   $^{56}\text{Ni}$ , the mass cut that separates the ejecta and the compact remnant should be as deep as  $M_{\text{cut}} \sim 1.4M_{\odot}$ . In the spherical model no fallback occurs. This suggests that the remnant was a neutron star rather than a black-hole. The mass range  $M_{\text{MS}} \sim 25M_{\odot}$  is near the transition from neutron star (SN 2005bf) to black hole formation (SN 2002ap; Mazzali et al. 2002), the exact boundary depending on rotation and mass loss.

Interestingly, the progenitor of the Cassiopeia A (Cas A) SN remnant was also probably a WN star, and its nucleosynthetic features are consistent with a  $\sim 25M_{\odot}$  star (e.g., Fesen et al. 2005 and references therein). The compact remnant of Cas A could be a magnetar (a neutron star with strong magnetic fields, Krause et al. 2005). The Cas A remnant is extremely clumpy, with many knots. The fastest Fe-rich ‘jet’ moves with  $v \sim 6,000 \text{ km s}^{-1}$  and is not mixed with N-He or O-rich layers (Fesen et al. 2005). These properties resemble our model for SN 2005bf. We might speculate that SN 2005bf was similar to the explosion of Cas A and that magnetorotational effects at collapse and later magnetar activity produced jets that created extremely clumpy ejecta in the  $^{56}\text{Ni}$ -rich layer. These jets were not energetic enough to reach the He layer.

Our best-fit model with enhanced  $\gamma$ -ray escape predicts that the apparent bolometric magnitude of SN 2005bf as it emerges from behind the Sun in late 2005 will be  $\sim 20.6$  (Fig. 2, inset). Without the enhanced  $\gamma$ -ray escape, this value would be  $\sim 19.0$  mag. SN 2005bf showed significant polarized spectral features (Wang & Baade 2005; Kawabata et al. 2005). Polarization observations (e.g., Kawabata et al. 2002) could be extremely useful to reveal the detailed distribution of the elements in the ejecta and the orientation of the possible jet, as would nebular spectra (Maeda et al. 2002; Mazzali et al. 2005).

This work has been supported in part by the Grant-in-Aid for Scientific Research (16540229, 17030005, 17033002) from the MEXT of Japan. Research on supernovae at Harvard University has been supported by NSF Grant AST-0205808. The

PAIRITEL is operated by the Smithsonian Astrophysical Observatory and a grant from the Harvard University Milton Fund.

## REFERENCES

- Anupama, G. C., Sahu, D. K., Deng, J., Nomoto, K., Tominaga, N., Tanaka, M., Mazzali, P. A., & Prabh, T. P. 2005, *ApJ*, 631, L125
- Arnett, W. D. 1982, *ApJ*, 253, 785
- Branch, D., et al., 2002, *ApJ*, 566, 1005
- Deng, J.S., Qiu, Y.L., Hu, J.Y., Hatano, K., & Branch, D. 2000, *ApJ*, 540, 452
- Ensmann, L.M., & Woosley, S.E. 1988, *ApJ*, 333, 754
- Falco, E.E., et al. 1999, *PASP*, 111, 438
- Fesen, R.A., et al. 2005, *ApJ*, in press (*astro-ph/0509067*)
- Folatelli, G., et al. 2005, *ApJ*, Submitted (*astro-ph/0509731*)
- Hamuy, M., Contreras, C., Gonzalez, S., Krzeminski, W. 2005, *IAU Circ.* 8520
- Harkness, R.P., et al. 1987, *ApJ*, 317, 355
- Hirschi, R., Meynet, G., & Maeder, A. 2005, *A&A*, 433, 1013
- Inada, N., et al. 2005, in preparation
- Iwamoto, K., et al. 2000, *ApJ*, 534, 660
- Kawabata, K., et al. 2002, *ApJ*, 580, L39
- Kawabata, K., et al. 2005, in preparation
- Krause, O., et al. 2005, *Science*, 308, 1604
- Lucy, L. B. 1991, *ApJ*, 383, 308
- Lucy, L. B. 1999, *A&A*, 345, 211
- Maeda, K., Nakamura, T., Nomoto, K., Mazzali, P.A., Patat, F., & Hachisu, I. 2002, *ApJ*, 565, 405
- Mazzali, P. A. & Lucy, L. B. 1993, *A&A*, 279, 447
- Mazzali, P. A. 2000, *A&A*, 363, 705
- Mazzali, P. A., Nomoto, K., Cappellaro, E., Nakamura, T., Umeda, H., & Iwamoto, K. 2001, *ApJ*, 547, 988
- Mazzali, P. A., et al. 2002, *ApJ*, 572, L61
- Mazzali, P. A., et al. 2005, *Science*, 308, 1284
- Modjaz, M., Kirshner, R., Challis, P., Matheson, T., & Landt, H., 2005a, *IAU Circ.* 8509
- Modjaz, M., Kirshner, R., & Challis, P. 2005b, *IAU Circ.* 8522
- Modjaz, M., et al. 2005c, in preparation
- Monard, L. A. G. 2005, *IAU Circ.* 8507
- Moore, M. & Li, W. 2005, *IAU Circ.* 8507
- Morrell, N., Hamuy, M., Folatelli, G., Contreras, C. 2005 *IAU Circ.* 8509
- Nakamura, T., Mazzali, P. A., Nomoto, K., Iwamoto, K. 2001, *ApJ*, 550, 991
- Nomoto, K., & Hashimoto, M. 1988, *Phys. Rep.*, 163, 13
- Nomoto, K., Iwamoto, K., & Suzuki, T. 1995 *Phys. Rep.*, 256, 173
- Nomoto, K., Maeda, K., Mazzali, P.A., Umeda, H., Deng, J., & Iwamoto, K. 2004, in *Stellar Collapse*, ed. C. L. Fryer (Kluwer: Dordrecht), 277 (*astro-ph/0308136*)
- Schlegel, D. J., Finkbeiner, D. P., & Davis, M. 1998 *ApJ*, 500, 525
- Shigeyama, T. & Nomoto, K. 1990, *ApJ*, 360, 242
- Umeda, H., & Nomoto, K. 2005, *ApJ*, 619, 427
- Wang, L., & Baade, D. 2005, *IAU Circ.* 8521
- Yoshii, Y. et al. 2003, *ApJ*, 592, 467

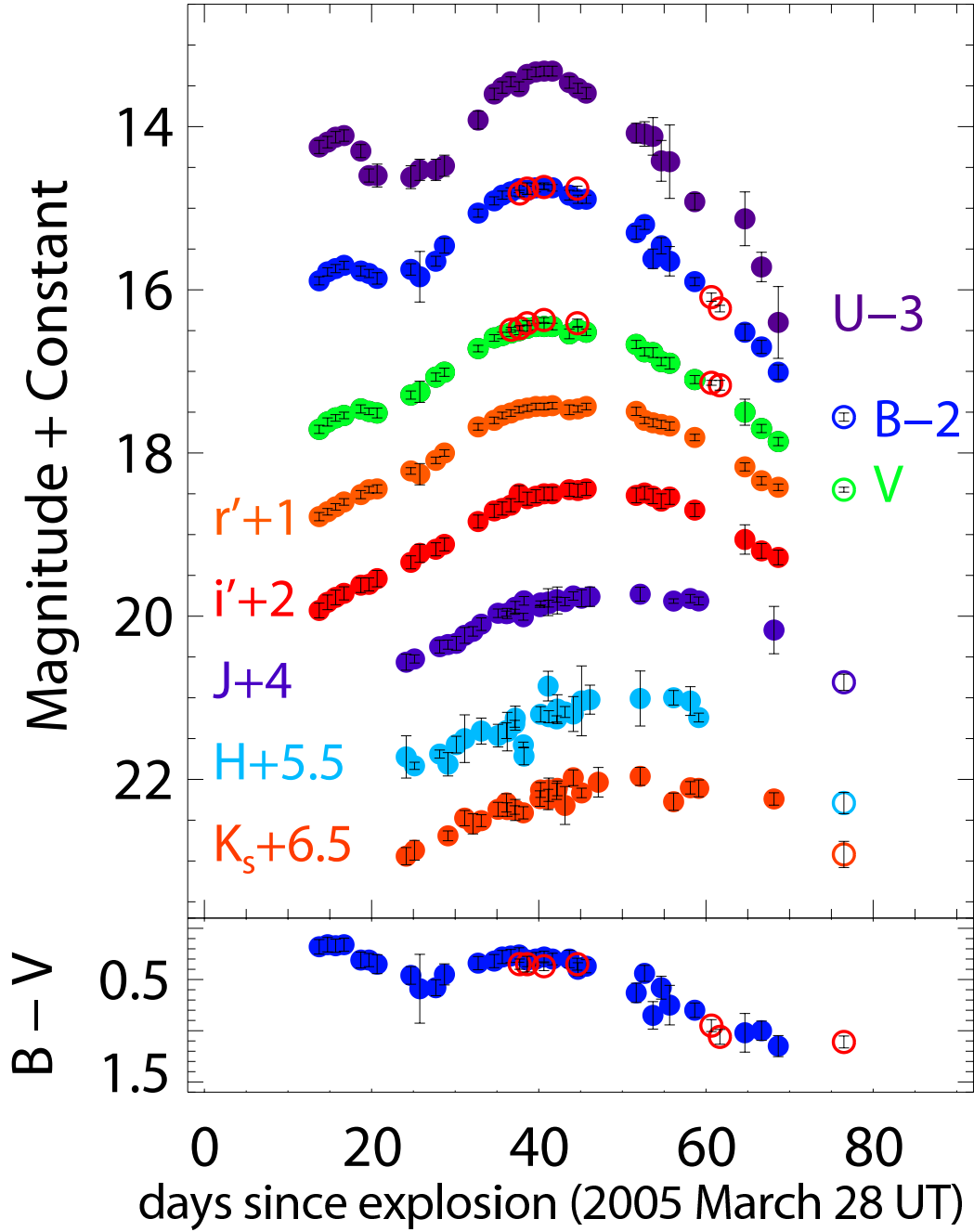


Fig. 1.— (top) Observed  $UBVr'i'JHK_s$  (or  $K$ ) light curve of SN 2005bf. Filled symbols are data from the Fred Lawrence Whipple Observatory (Modjaz et al. 2005c), open symbols are data from the Himalayan Chandra Telescope and the MAGNUM Telescope (Anupama et al. 2005; Inada et al. 2005). (bottom) Observed  $B - V$  color evolution. The meaning of the symbols is the same as in the top panel.

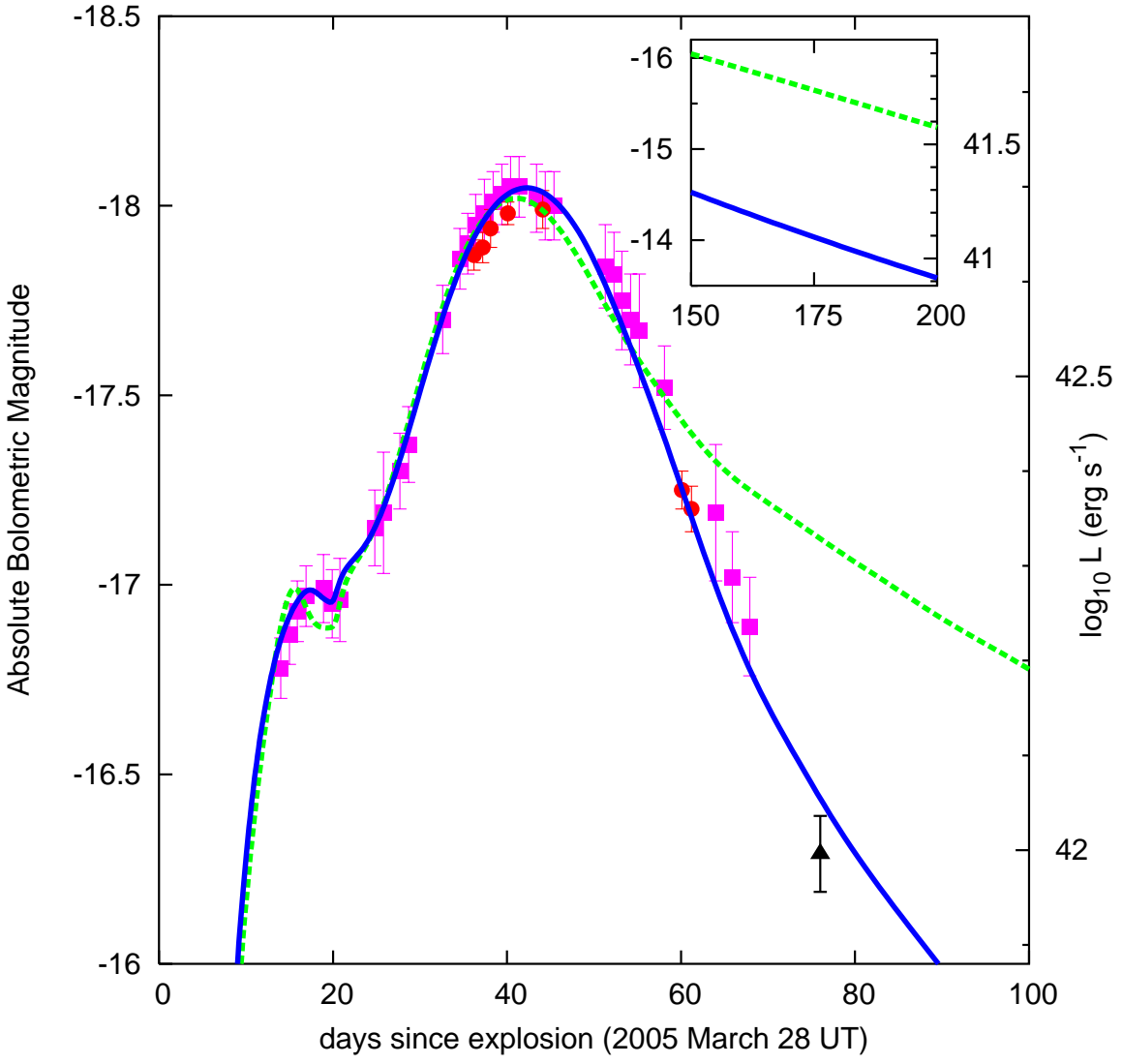


Fig. 2.— The bolometric light curve constructed from FLWO (filled squares; Modjaz et al. 2005c), HCT (filled circles; Anupama et al. 2005), and MAGNUM (filled triangle; Inada et al. 2005) photometry. The contribution of near-IR light is between  $\sim 20\%$  of the total at early phases to  $\sim 50\%$  at late phases. Synthetic light curves are shown for normal (dashed) and reduced (solid)  $\gamma$ -ray opacities (see text). The inset shows the predicted LCs of each model when SN 2005bf emerges from behind the Sun in fall 2005.

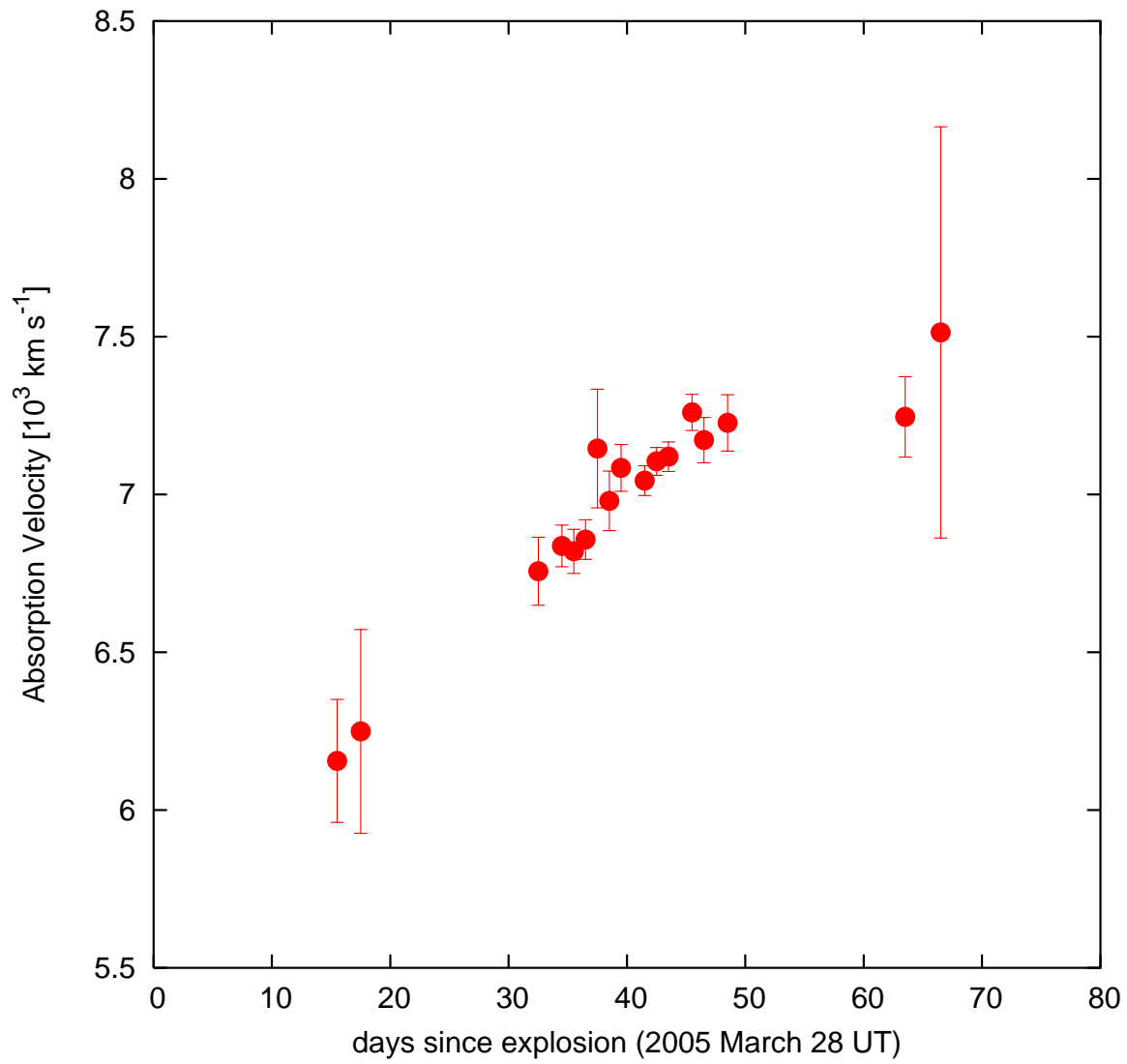


Fig. 3.— The time evolution of the He line velocity derived from the absorption minimum of He I  $\lambda$  5876 (Modjaz et al. 2005c).

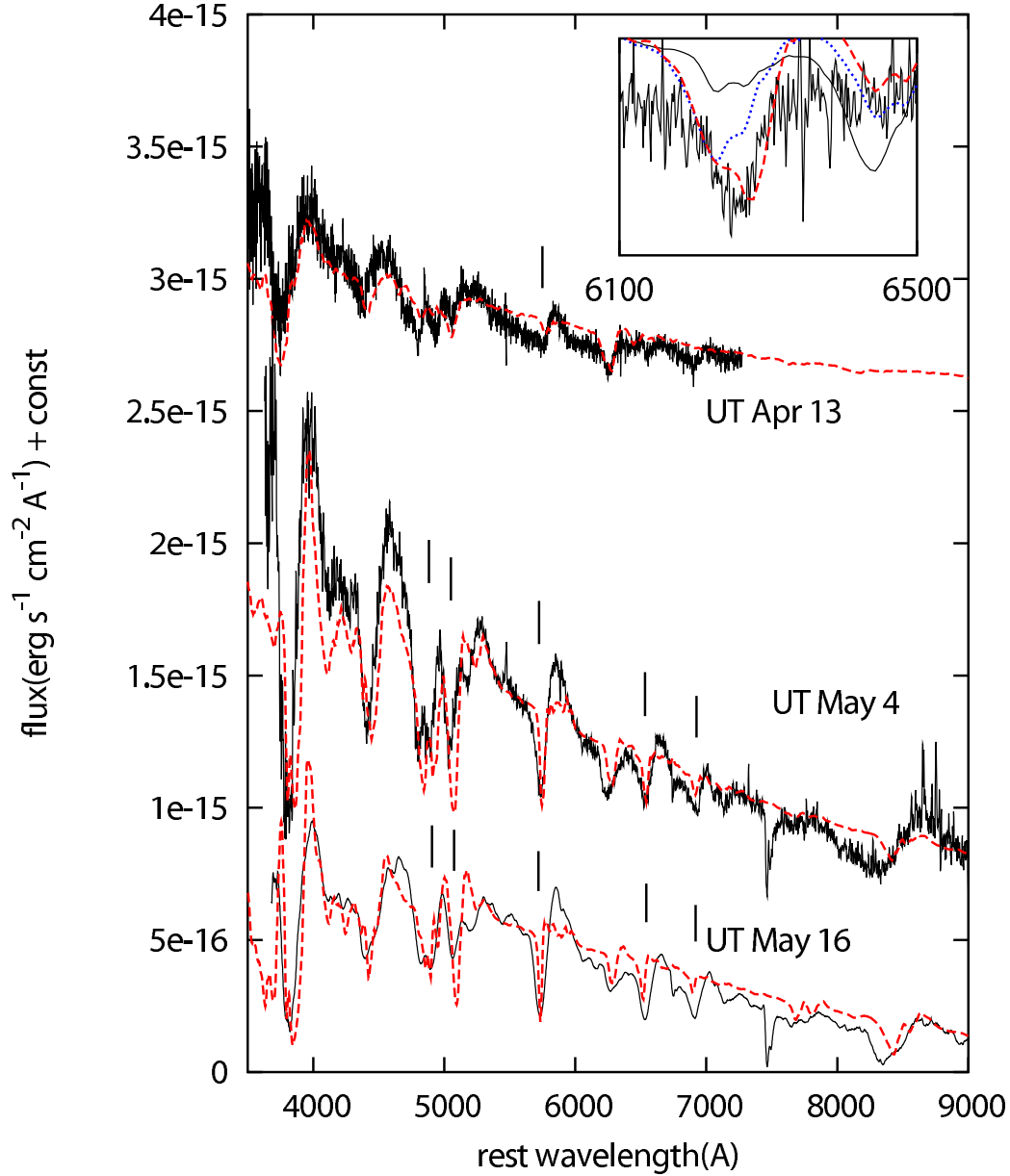


Fig. 4.— Spectra of SN 2005bf (thick lines: 2005 April 13 - FLWO, Modjaz et al. 2005c; May 4 - HCT, Anupama et al. 2005; May 16 - Subaru Telescope, Kawabata et al. 2005) compared to the synthetic spectra (dashed lines) computed with the model  $(M_{ej}/M_{\odot}, E_{51}) = (7, 1.3)$ . The position of He lines is shown by tick marks. The absorptions near 4900 and 5100Å are blended with Fe II lines. The inset shows the absorption near 6300Å in the April 13th spectrum. The model with H at  $v \gtrsim 13,000 \text{ km s}^{-1}$  (dashed line) provides the best fit. Thin and dotted lines show models with H in the whole ejecta and no H, respectively.